© 2017. Published by The Company of Biologists Ltd | Journal of Experimental Biology (2017) 220, 3053-3061 doi:10.1242/jeb.159764

RESEARCH ARTICLE

# The tendinopathic Achilles tendon does not remain iso-volumetric upon repeated loading: insights from 3D ultrasound

**Leila Nuri[1,*], Steven J. Obst[2], Richard Newsham-West[1] and Rod S. Barrett[1]**

## ABSTRACT

Mid-portion Achilles tendinopathy (MAT) alters the normal three-dimensional (3D) morphology of the Achilles tendon (AT) at rest and under a single tensile load. However, how MAT changes the 3D morphology of the AT during repeated loading remains unclear. This study compared the AT longitudinal, transverse and volume strains during repeated loading of the tendinopathic AT with those of the contralateral tendon in people with unilateral MAT. Ten adults with unilateral MAT performed 10 successive 25 s submaximal (50%) voluntary isometric plantarflexion contractions with both legs. Freehand 3D ultrasound scans were recorded and used to measure whole AT, free AT and proximal AT longitudinal strains and free AT cross-sectional area (CSA) and volume strains. The free AT experienced higher longitudinal and CSA strain and reached steady state following a greater number of contractions (five contractions) in the tendinopathic AT compared with the contralateral tendon (three contractions). Further, free tendon CSA and volume strain were greater in the tendinopathic AT than in the contralateral tendon from the first contraction, whereas free AT longitudinal strain was not greater than that of the contralateral tendon until the fourth contraction. Volume loss from the tendon core therefore preceded the greater longitudinal strain in the tendinopathic AT. Overall, these findings suggest that the tendinopathic free AT experiences an exaggerated longitudinal and transverse strain response under repeated loading that is underpinned by an altered interaction between solid and fluid tendon matrix components. These alterations are indicative of accentuated poroelasticity and an altered local stress–strain environment within the tendinopathic free tendon matrix, which could affect tendon remodelling via mechanobiological pathways.

**KEY WORDS: Creep, Strain, Cross-sectional area, Mid-portion Achilles tendinopathy, Volume, Free tendon**

## INTRODUCTION

Mid-portion Achilles tendinopathy (MAT) is a common pathology of the lower extremity that is characterized by pain, swelling and thickening of the Achilles tendon (AT) mid-portion (Maffulli et al., 1998; Van Dijk et al., 2011). MAT affects sporting and general populations, causing disability, functional impairment and compromised performance (Kvist, 1994; De Jonge et al., 2011). MAT has been shown to result in altered tendon composition, structure and morphology, including an increase in tendon cross-sectional area (CSA), thickness and volume (Shalabi et al., 2004; Arya and Kulig, 2010; Child et al., 2010; Grigg et al., 2012; Docking and Cook, 2016). The tendinopathic AT also exhibits lower stiffness and Young's modulus as well as greater longitudinal and transverse strains and higher hysteresis compared with healthy tendon under the same tensile load (Arya and Kulig, 2010; Child et al., 2010; Wang et al., 2012; Chang and Kulig, 2015). Alterations in AT geometry and material properties in MAT are important because of their potential to change the stress–strain patterns experienced by the AT during muscle contraction (Hansen et al., 2017). It has also been shown that in contrast to healthy tendon, which bulges along the antero-posterior diameter (Obst et al., 2014b, 2015) and experiences a reduction in CSA and behaves iso-volumetrically (Obst et al., 2014b, 2015; Nuri et al., 2016) during a single tensile load, the tendinopathic tendon undergoes a reduction in antero-posterior diameter and CSA and a corresponding reduction in volume of the tendon core. This observation is suggestive of fluid exudation from the tendon core (i.e. the whole tendon, covered by the epitenon layer) to the peritendinous space (i.e. the space between the tendon epitenon and paratenon layers) and tendon matrix re-organization under load in MAT. To our knowledge, no *in vivo* studies to date have examined the time-dependent visco-poroelastic properties of MAT during repeated loading. Such studies could provide an insight into the time scale of interaction and involvement of tendon load-bearing components [solid (i.e. collagen fibrillar network and proteoglycans) and fluid (i.e. water)] within the tendinopathic tendon matrix during repeated loading.

*In vivo* studies of the time-dependent viscoelastic properties of the AT to date have been confined to normal tendon. In general, these studies show that during repeated application of the same force, the normal AT experiences gradual 3D deformation (i.e. creep) until steady-state behaviour is reached (Fung, 2013). For example, Maganaris (2003) reported that high-intensity (80%) successive maximal voluntary isometric contraction (MVIC) of the plantarflexors induced ∼5 mm increase in whole AT [e.g. gastrocnemius muscle–tendon junction (MTJ) to calcaneus] longitudinal elongation that reached steady-state behaviour after five contractions. Similarly, Hawkins et al. (2009) showed that low-intensity repeated isometric contractions (25–35% MVIC) resulted in ∼3% increase in whole AT longitudinal strain that plateaued after 270 contractions. More recently, Nuri et al. (2016) reported that whole AT longitudinal and transverse deformation during repeated loading were primarily driven from free AT (e.g. soleus MTJ to calcaneus), with little or no contribution from proximal AT (e.g. gastrocnemius MTJ to soleus MTJ) in healthy people and that both longitudinal and transverse deformation of the free AT reached steady state after three repetitions of a 25 s submaximal (50% MVIC) isometric plantarflexion contraction. As healthy free AT behaved iso-volumetrically during repetitive contractions, the

[1]School of Allied Health Sciences, Menzies Health Institute Queensland, Griffith University, Gold Coast, QLD 4222, Australia. [2]School of Health, Medical and Applied Sciences, Central Queensland University, Bundaberg, QLD 4670, Australia.

*Author for correspondence (leila.nuri@griffithuni.edu.au)

L.N., 0000-0001-5798-626X

**Received 20 March 2017; Accepted 12 June 2017**

Journal of Experimental Biology (2017) 220, 3053-3061 doi:10.1242/jeb.159764

alterations in tendon longitudinal and transverse morphologies during the first three contractions were indicative of a change in tendon matrix shape, with increased tendon length coupled to the reduction in tendon CSA (Nuri et al., 2016).

In contrast to healthy tendon, the loss of free AT volume during acute loading in MAT suggests that the normal interaction between solid and fluid matrix components may be interrupted. A continued loss of free tendon volume in MAT with repeated loading might be expected to increase loading on the solid component of the tendon matrix and adversely affect the ability of the tendon to resist ongoing loading. A loss of tendon volume with repeated loading could therefore be an important factor that limits tendon function and repair in tendinopathy as a result of the effect on the local tendon mechanobiology. Assessing changes in tendinopathic tendon morphology and volume during repeated loading may also provide an indication of the temporal relationship between collagen creep and fluid exudation from the tendon core in MAT. This knowledge could also inform computational models of poroelastic tendon behaviour in tendinopathy (Smith et al., 2013) and be useful for establishing a standardized conditioning protocol for individuals with MAT prior to performing mechanical tests, treatment protocols and physical activity. A greater number of contractions to reach steady-state behaviour might be expected in MAT because of the dual and interacting effects of changes in solid and fluid matrix component behaviour.

The purpose of the present study was therefore to investigate the effect of repeated submaximal isometric plantarflexion contractions on the longitudinal deformation of the whole AT and the corresponding free tendon transverse and volume deformation of the tendinopathic side relative to those of the contralateral side in people with unilateral MAT. We hypothesized that longitudinal, transverse and volume strains would reach steady state at a higher magnitude and following a greater number of contractions in the tendinopathic AT compared with the contralateral tendon. We also sought to determine whether the time-dependent viscoelastic properties in MAT are mainly driven from the free AT as in normal tendon (Nuri et al., 2016), or whether the proximal AT exhibits altered behaviour in MAT.

## MATERIALS AND METHODS

### Participants

Ten individuals with MAT participated in the study. The inclusion criteria were: male adults, 18–60 years of age with unilateral MAT, duration of pain greater than 3 months and VISA-A score (Victorian Institute of Sports Assessment-Achilles tendon score, an index of the severity of Achilles tendinopathy, 0–100) of less than 80 points (Alfredson et al., 1998; Debenham et al., 2016). The exclusion criteria were: insertional tendinopathy, bilateral tendinopathy, history of AT rupture or surgery, inflammatory or degenerative ankle joint condition, and any musculoskeletal injuries thought to interfere with participation in the study. All clinical examinations were performed by the same physiotherapist (L.N.). Participant characteristics were: age 42.2±11.5 years, height 176.6±7.5 cm, mass 79.8±7.8 kg, VISA-A score 54.2±16.5, and duration of symptoms 3.5±2 years. All the participants provided written informed consent before participation. The study was approved by the Griffith University human research ethics committee and was performed in accordance with the principles of the Declaration of Helsinki.

### Experimental protocol

Following the clinical examination, participants completed a familiarization session on the same day and a testing session 3–5 days later. In the familiarization session, each participant performed three repetitions of a 4 s MVIC of the plantarflexors and dorsiflexors separately for each leg on the apparatus described below. A rest period of 60 s was allowed between contractions. The contraction with the highest torque on the tendinopathic side was chosen to determine the target torque (50% MVIC) for both legs in the subsequent testing session. Participants were then asked to practice holding contractions at 50% MVIC until they became familiarized with the testing procedure.

Participants were instructed to refrain from any form of training or vigorous physical activity for at least 48 h prior to the subsequent testing session and to use motorized transportation to travel to the laboratory. Upon arrival participants rested on a chair for 45 min (Nuri et al., 2016) and were subsequently asked to lie prone on an examination plinth with their knee and hip fully extended, and the ankle joint in neutral position. Their foot was then firmly secured to a footplate connected to a fixed torque transducer (TFF600, Futek, Irvine, CA, USA) using a custom-made adjustable ratchet system to minimize heel lift from the footplate during contractions (Obst et al., 2014a,b). The rotational axis of the torque transducer was carefully aligned with the axis of rotation of the ankle joint. Visual feedback of the torque exerted by the foot was provided on a computer monitor, positioned 1 m directly in front of the participants at eye level. The output from the torque transducer was recorded at a sampling frequency of 1000 Hz through LabVIEW software (v9.9, National Instruments, Austin, TX, USA). Participants performed 10 successive isometric plantarflexion contractions at 50% MVIC with both legs separately. The order of testing of the legs (tendinopathic or contralateral side) was randomly decided for each participant. Verbal encouragement was provided to participants during each contraction. Pain was assessed during each contraction using a 10 cm visual analogue scale (VAS), with 0 indicating no pain and 10 indicating the worst possible pain for each leg separately. Prior to testing, all participants were familiarized with the use of the VAS scoring system and were instructed to circle a number on the scale that corresponded to the pain in the AT following each contraction.

### Freehand 3D ultrasound

Ultrasound scans were acquired at two resting states (e.g. immediately before the first contraction and immediately after completing the tenth contraction) and during each of 10 contractions using a freehand 3D ultrasound system (US) consisting of a conventional ultrasound machine (SonixTouch, Ultrasonix, Richmond, BC, Canada) and a five-camera optical tracking system (V100:R2, Tracking Tools v2.5.2, Natural Point, Corvallis, OR, USA) (Obst et al., 2014a). The 3D position and orientation of the ultrasound transducer were determined from four reflective markers rigidly attached to the transducer using the optical tracking system. A coordinate transformation was then used to map the 2D brightness-mode (B-mode) ultrasound images to a global coordinate system and a 3D reconstruction of the AT was created using the Stradwin software package (v5.1, Mechanical Engineering, Cambridge University, UK; http://mi.eng.cam.ac.uk/~rwp/stradwin/). Before data collection, the temporal and spatial calibration of the ultrasound transducer was performed in a water bath (~25°C) using a single-wall phantom calibration protocol recommended by Stradwin software developers (Prager et al., 1998). After calibration, pixel coordinates in any recorded 2D ultrasound images were transformed into 3D space with an approximate error of ±0.4 mm (Prager et al., 1998).

One investigator (L.N.) performed all the AT ultrasound scans using a 58 mm linear transducer (L14-5 W/60 linear, Ultrasonix)

Journal of Experimental Biology (2017) 220, 3053-3061 doi:10.1242/jeb.159764

with standardized ultrasound image settings (depth 40 mm, gain 50%, dynamic range 65 dB, map 4, power 0). To ensure a consistent scanning area for all the contractions, the ultrasound scanning area was drawn on the skin according to the AT anatomical location seen with 2D real-time ultrasound (Fig. 1A). A rectangular commercially available stand-off pad was attached to the end of the transducer using a custom-made ultrasound stand-off holder to maximize the image quality. A thick layer of ultrasound gel was then applied over the AT scanning area in order to provide appropriate ultrasound wave conductance and minimize the pressure exerted by the transducer on the skin. A stack of 2D B-mode images was then acquired by moving the transducer manually from the base of the heel to the medial gastrocnemius (MG) MTJ in a transverse orientation at a steady speed (~9 mm $s^{-1}$). Each ultrasound scan took approximately 25 s to complete and the finalized stacks of 2D B-mode images consisted of 1350 frames with an average distance frame of 0.1 mm. The 3D US approach is limited to evaluating tendon morphology under the static loading condition and the accuracy of measurement, particularly for tendon length, depends on the scanning time and the number of 2D B-mode images acquired during scanning (Lichtwark et al., 2013; Obst et al., 2014a). Therefore, the tendon loading condition under which the AT ultrasound scanning was performed in the present study (i.e. ~25 s isometric plantarflexion contraction at 50% MVIC) was a compromise between allowing sufficient scan time to capture a sufficiently dense ultrasound image stack, and ensuring that participants were able to maintain the target contraction intensity over the scan period (Nuri et al., 2016).

Three main anatomical point landmarks [calcaneal notch, soleus (SOL) MTJ and MG MTJ] were selected manually on 3D AT images using the 3D landmark tool in Stradwin software. Sagittal and frontal image re-slices were used to start the manual segmentation and were corrected where necessary by viewing the corresponding 3D transverse image slices (Fig. 1B,C). The whole AT length was defined as the distance between the calcaneal notch and the MG MTJ; the free AT length was defined as the distance between the calcaneal notch and the SOL MTJ; and proximal AT length was defined as the distance between the MG MTJ and SOL MTJ. Tendon deformation was determined by subtracting tendon resting length from the corresponding length during each contraction. Sagittal and

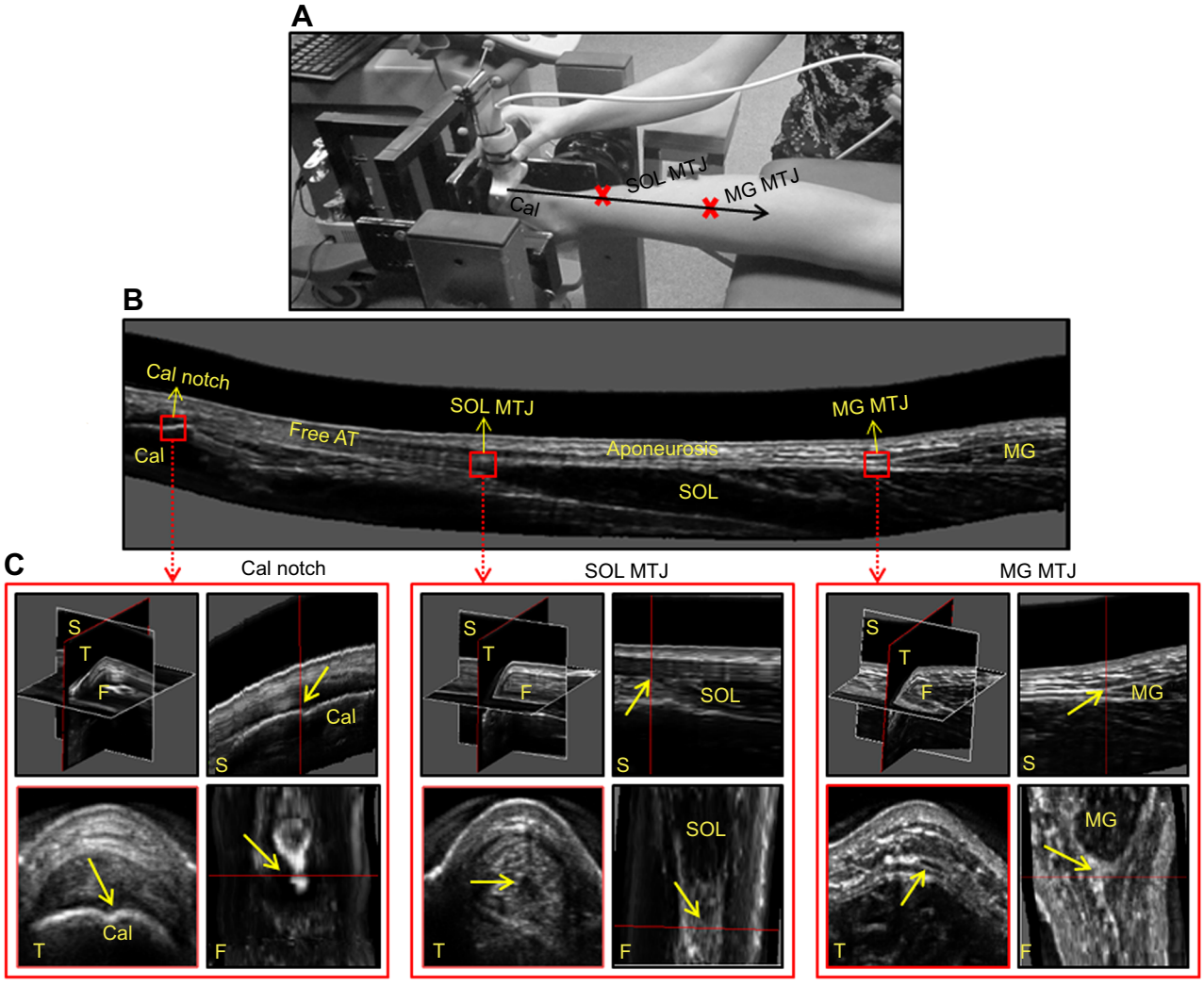


**Fig. 1. Experimental set-up and three dimensional (3D) Achilles tendon (AT) image reconstruction and segmentation.** (A) A participant positioned prone in the testing apparatus with the ankle joint at 90 deg (neutral position). The ultrasound scan was performed by sweeping the ultrasound transducer from the base of the heel to the medial gastrocnemius (MG) muscle–tendon junction (MTJ) as indicated by the arrow. The crosses denote MTJ for the soleus (SOL) and MG. Cal, calcaneus. (B) Sagittal plane re-slices of the reconstructed 3D ultrasound image of the AT. (C) Sagittal (S), transverse (T) and frontal (F) image re-slices used to identify the anatomical location of the calcaneal (Cal) notch, SOL MTJ and MG MTJ.



Journal of Experimental Biology

Journal of Experimental Biology (2017) 220, 3053-3061 doi:10.1242/jeb.159764

transversal images of free tendon were used to digitize tendon CSA at 2 mm intervals along the length of the free tendon. The free AT volume reconstruction was then obtained from the 3D location of the digitized CSAs using 3D rendering algorithms in Stradwin (Treece et al., 1999) (Fig. 2). The accuracy of our 3D US for free AT volume measurement compared with phantoms of similar size and the minimal detectable change for *in vivo* free AT volume at rest have been estimated to be ±0.5 ml and ±0.2 ml, respectively (Obst et al., 2014a). Further, 3D US provides a high level of within-session reliability (intraclass correlation ≥0.98) for the measures of AT morphological properties (i.e. AT length, mean free AT CSA, and free AT volume) at rest and during sub-maximal voluntary isometric plantarflexion contraction (Obst et al., 2014a; Nuri et al., 2016). The mean free tendon CSA ($mm^2$) was obtained by dividing free tendon volume by free tendon length (×1000). Tendon length, CSA and volume strains were computed by dividing the tendon deformation by the corresponding resting values.

### Electromyography (EMG)

Following skin preparation, pre-gelled and self-adhesive surface electrodes (model H124SG, 24 mm, Covidien Kendall, Neustadt, Germany) with a fixed centre-to-centre interelectrode distance of 20 mm were placed over the belly of the MG, lateral gastrocnemius (LG), SOL and tibialis anterior (TA) muscles according to SENIAM recommendations by Hermens et al. (2000). A ground reference electrode was placed over the fibular head. Muscle activity was recorded using a four-channel double differential EMG system (Bagnoli-8 EMG, Delsys, Natick, MA, USA). EMG signals were sampled at a frequency of 1000 Hz and bandpass filtered between 20 and 400 Hz using a fourth-order zero-lag Butterworth filter in Matlab software (The Mathworks, Natick, MA, USA) and converted to root mean square (RMS) values. The RMS value was then normalized relative to the measured MVIC values (% MVIC). EMG activity for MG, LG and SOL was also expressed as a ratio of total triceps surae (TS) muscle activation to investigate the effects of each contraction on the synergetic activations. Furthermore, the co-activation index was calculated from the ratio of normalized EMG activity for TA to the sum of normalized EMG activities for the SOL and TA (Hammond et al., 1988).

### Statistical analysis

Paired *t*-tests were used to compare the resting dimensions of the tendon (whole AT, free AT and proximal AT lengths, and free AT CSA and volume) between sides (tendinopathic and contralateral). A full-factorial two-way repeated measures ANOVA was used to evaluate the effects of side and contraction number (10 contractions) on tendon longitudinal strain for each tendon region (whole AT, free AT and proximal AT), free tendon CSA strain and free tendon volume strain separately. Planned contrasts (SPSS CONTRAST syntax) were subsequently used to determine differences in tendon longitudinal strain, CSA strain and volume strain between sides for each contraction and between consecutive contractions for each side. Furthermore, a one-way repeated measures ANOVA was used to determine the effect of contraction number on ankle joint torque, pain score, EMG activity of MG, LG, SOL and TA muscles, the ratios of normalized EMG activity, and the co-activation index for each side separately. The level of significance was set at $\alpha$=0.05. All analyses were performed using the Statistical Package for the Social Sciences v22 (SPSS, Chicago, IL, USA). In the text, data are expressed as means±s.d. and in the figures they are presented as means±s.e.m.

## RESULTS

### Effect of tendon side on tendon dimensions at rest

No differences in resting lengths of tendon regions were detected between the tendinopathic side (whole AT: 203±29 mm; free AT: 74±23 mm; proximal AT: 129±23 mm) and the contralateral side (whole AT: 206±23 mm; free AT: 72±22 mm; proximal AT: 134±21 mm) ($t_9$=−0.04, $P$=0.96; $t_9$=−0.84, $P$=0.41; $t_9$=1.02, $P$=0.33, respectively). However, the mean resting free AT CSA was significantly higher for the tendinopathic side (97±17 $mm^2$) compared with the contralateral side (60±13 $mm^2$) ($t_9$=−8.63, $P$<0.001). Similarly, the mean resting free AT volume was significantly higher for the tendinopathic side (7.16±1.89 ml) compared with the contralateral side (4.15±1.01 ml) ($t_9$=−8.84, $P$<0.001).

### Effect of tendon side and contraction number on AT longitudinal strain

The whole AT, free AT and proximal AT longitudinal elongations and the corresponding strains are displayed in Fig. 3. Significant

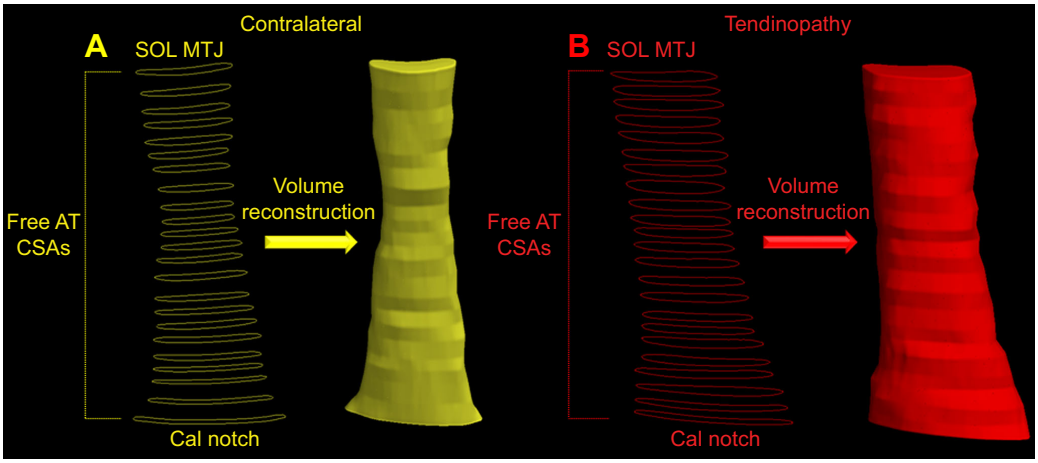


**Fig. 2. Free AT cross-sectional area (CSA) segmentation and volume reconstruction for contralateral and tendinopathic sides of a single representative participant.** (A) Contralateral AT. (B) Tendinopathic AT. The free AT CSAs were manually digitized from the transverse images at 2 mm intervals from the calcaneal (Cal) notch to the SOL MTJ and the free AT 3D volume was rendered from the segmented CSAs using the surface interpolation algorithm in Stradwin software.



Journal of Experimental Biology

Journal of Experimental Biology (2017) 220, 3053-3061 doi:10.1242/jeb.159764

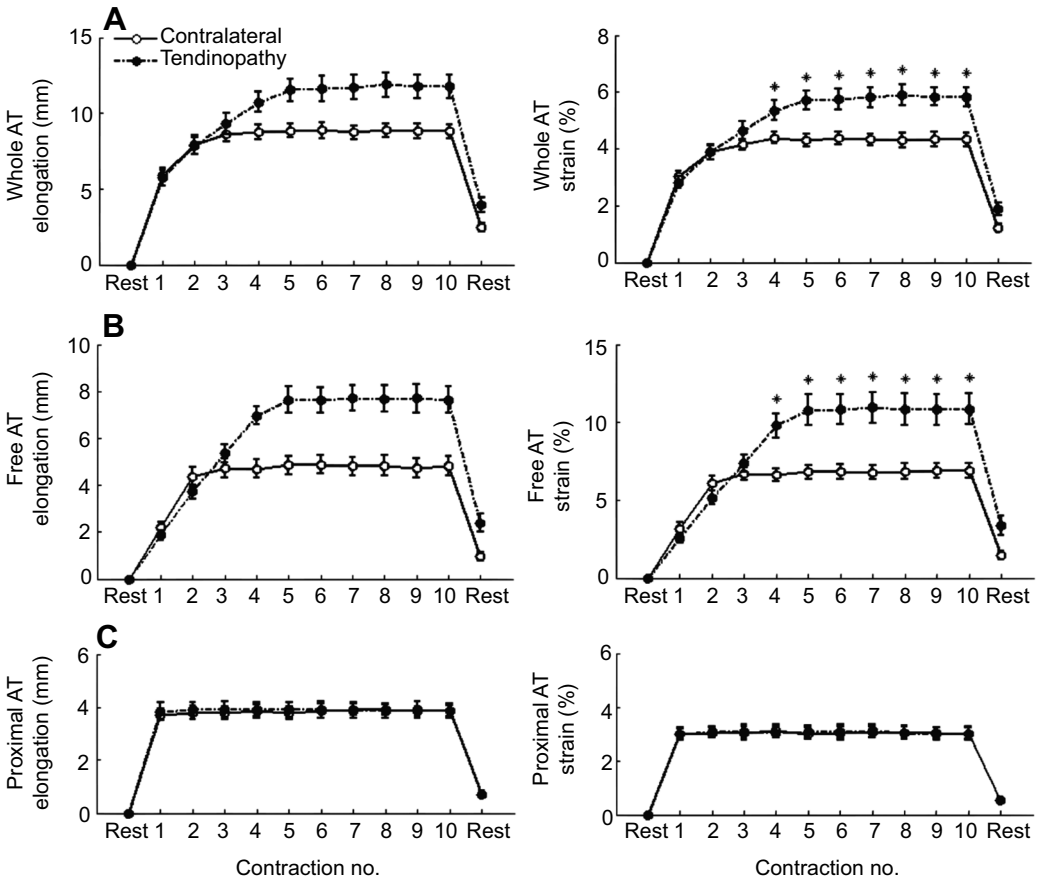


**Fig. 3. Change in AT longitudinal elongation and strain during repeated loading.** The mean group whole AT (A), free AT (B) and proximal AT (C) longitudinal elongation and strain of the tendinopathic and contralateral sides during 10 successive isometric plantarflexion contractions at 50% maximal voluntary isometric contraction (MVIC). Data are expressed as means±s.e.m. ($n$=10). Asterisks indicate significant differences between the tendinopathic and contralateral sides during each contraction ($P$<0.05). Planned contrasts revealed that the whole and free AT of the tendinopathic side experienced greater longitudinal strain than those of the contralateral side during contractions 4–10.

main effects of side and contraction number were detected for whole AT longitudinal strain ($F_{1,9}$=7.37, $P$=0.02 and $F_{9,81}$=49.04, $P$<0.001, respectively) and free AT longitudinal strain ($F_{1,9}$=25.61, $P$=0.001 and $F_{9,81}$=74.76, $P$<0.001, respectively). Significant side-by-contraction number interaction effects were also detected for whole and free AT longitudinal strain ($F_{9,81}$=15.21, $P$<0.001 and $F_{9,81}$=25.35, $P$<0.001, respectively). Planned contrasts revealed greater whole and free AT longitudinal strain in the tendinopathic versus contralateral side from the fourth contraction. Planned contrasts also revealed that whole and free

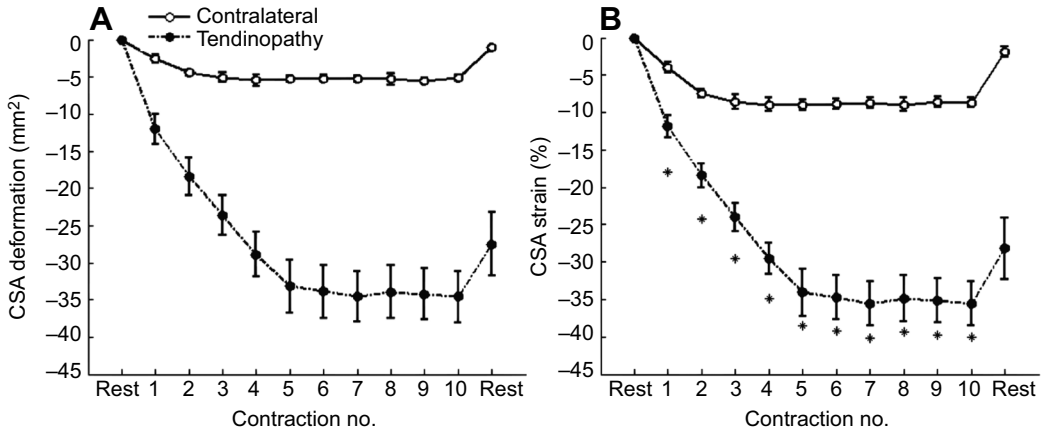


**Fig. 4. Change in free AT CSA deformation and strain during repeated loading.** The mean group free AT CSA deformation (A) and strain (B) during 10 successive isometric plantarflexion contractions at 50% MVIC of the tendinopathic and contralateral sides. Data are expressed as means±s.e.m. ($n$=10). Asterisks indicate significant differences between the tendinopathic and contralateral sides during each contraction ($P$<0.05). Planned contrasts revealed that the free tendon CSA of the tendinopathic side experienced greater strain than that of the contralateral side during contractions 1–10.

Journal of Experimental Biology (2017) 220, 3053-3061 doi:10.1242/jeb.159764

AT longitudinal strain values increased as a function of contraction number up to the fifth contraction in the tendinopathic side and the third contraction in the contralateral side for both regions (Fig. 3A,B). No significant differences in proximal AT strain were found between contractions in the two sides (Fig. 3C).

### Effect of tendon side and contraction number on free tendon transverse strain

The free AT CSA deformation and the corresponding strain are presented in Fig. 4. Side and contraction number had a significant main effect on mean free AT CSA strain ($F_{1,9}$=11.05, $P$=0.009 and $F_{9,81}$=23.73, $P$<0.001, respectively). A significant side-by-contraction number interaction for free AT CSA strain was also detected ($F_{9,81}$=6.79, $P$<0.001). Planned contrasts revealed that free AT CSA strain was significantly greater for the tendinopathic side compared with the contralateral side during all 10 contractions. Planned contrasts also revealed that free AT CSA strain values significantly decreased with contraction number up to the fifth contraction on the tendinopathic side and the third contraction on the contralateral side (Fig. 4B).

### Effect of tendon side and contraction number on free tendon volume strain

The free AT volume deformation and the corresponding strain are displayed in Fig. 5. Side and contraction number had a significant main effect on mean free AT volume ($F_{1,9}$=94.36, $P$<0.001 and $F_{9,81}$=19.59, $P$<0.001, respectively). There was a significant side-by-contraction number interaction for free AT volume strain ($F_{9,81}$=18.11, $P$<0.001). Planned contrasts revealed that free AT volume strain was significantly greater for the tendinopathic side compared with the contralateral side during all 10 contractions. Planned contrasts also revealed that free AT volume strain values significantly decreased with contraction number up to the fifth contraction in the tendinopathic side (Fig. 5B).

### Effect of contraction number on ankle joint torque, EMG and pain score

Ankle plantarflexion torque for MVIC on the tendinopathic side was 90.5±10.35 N m and for submaximal contractions on the tendinopathic and contralateral sides it was 45.77±4.22 and 44.52±5.25 N m, respectively. Normalized EMG activities for MG, LG, SOL and TA for the tendinopathic side were 38.34±3.81%, 21.93±2.21%, 36.34±1.23% and 5.55±0.32%, respectively, and for the contralateral side were 39.23±0.76%, 25.11±1.58%, 38.61±0.79% and 5.42±0.85%, respectively. The co-activation index for the tendinopathic and contralateral sides was 0.12±0.008 and 0.11±0.006, respectively. No significant main effects of contraction number or differences in ankle joint torque, normalized EMG activity of MG, LG, SOL and TA, ratios of normalized EMG activity (MG/TS, LG/TS, SOL/TS), and co-activation index between contractions were detected for the two sides. The group mean pain score during 10 contractions for the tendinopathic and contralateral sides was 1.5±0.46 and 0.02±0.03, respectively. There was a significant difference in tendon pain score between contractions for the tendinopathic side ($F_{9,81}$=12.32, $P$<0.001). Planned contrast revealed that tendon pain decreased from contraction 1 (2.6±1.5) to 2 (1.82±1.14) and from contraction 2 to 3 (1.35±0.85). No significant difference in tendon pain score was found between contractions for the contralateral side.

## DISCUSSION

This study examined the time course of longitudinal deformation of the whole AT, free AT and proximal AT, and the transverse and volume deformation of the free AT in people with unilateral MAT during repeated submaximal isometric plantarflexion contractions. Our hypothesis that AT longitudinal, transverse and volume strains would be greater and would require a greater number of contractions to reach steady state in the tendinopathic AT compared with contralateral tendon was supported. The volume reduction due to repeated loading preceded the exaggerated longitudinal strain response in MAT, and is suggestive of fluid loss from the tendon core. The observed rapid volume loss coupled with the aberrant 3D strain behaviour of the free AT in MAT are indicative of accentuated poroelasticity and an altered local stress–strain environment within the free tendon in tendinopathy, which could alter tendon remodelling via mechanobiological pathways.

### Resting CSA and volume of the tendinopathic and contralateral free AT

Consistent with previous *in vivo* studies, the tendinopathic side had a larger mean resting free AT CSA than the contralateral tendon (97 and 60 mm$^2$, respectively) (Leung and Griffith, 2008; Arya and

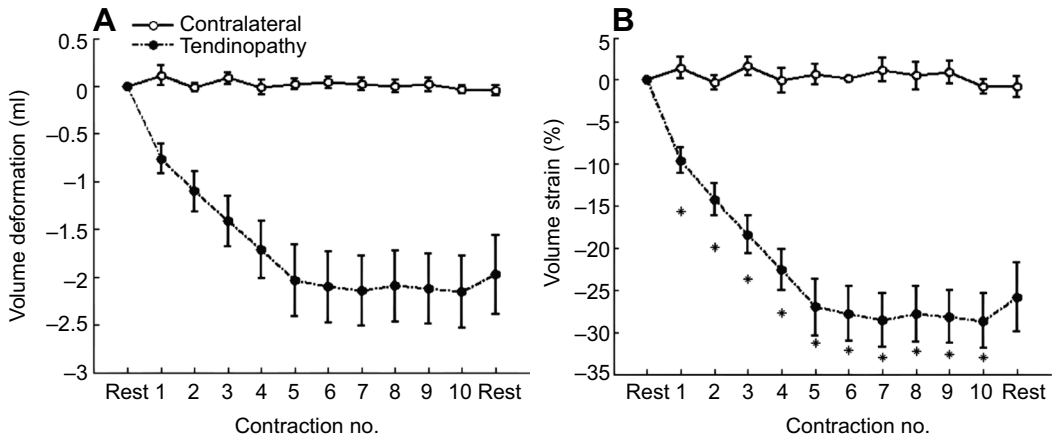


**Fig. 5. Change in free AT volume deformation and strain during repeated loading.** The mean group free AT volume deformation (A) and strain (B) during 10 successive isometric plantarflexion contractions at 50% MVIC of the tendinopathic and contralateral sides. Data are expressed as means±s.e.m. ($n$=10). Asterisks indicate significant differences between the tendinopathic and contralateral sides during each contraction ($P$<0.05). Planned contrasts revealed that the free tendon volume of the tendinopathic side experienced greater strain than that of the contralateral side during contractions 1–10.



Journal of Experimental Biology

Journal of Experimental Biology (2017) 220, 3053-3061 doi:10.1242/jeb.159764

Kulig, 2010; Docking and Cook, 2016), reflecting the pathological alterations in tendon structure and composition within MAT. The mean resting free tendon CSA value reported here for the tendinopathic AT (97 $mm^2$) lies within the range of values reported in previous studies for free AT in individuals with MAT (90–100 $mm^2$) (Leung and Griffith, 2008; Arya and Kulig, 2010; Docking and Cook, 2016). The mean resting contralateral free tendon CSA value in the present study (60 $mm^2$) was also in close agreement (56–75 $mm^2$) with prior studies using the same approach (Obst et al., 2015; Nuri et al., 2016), but was lower than that for several prior studies (80–90 $mm^2$) (Maganaris and Paul, 2002; Magnusson and Kjaer, 2003; Reeves and Cooper, 2017). We believe this discrepancy in normal tendon CSA between studies could be due to the differences in imaging methods [MRI (Magnusson and Kjaer, 2003; Reeves and Cooper, 2017); 2D US (Maganaris and Paul, 2002); 3D US (present study)], tendon CSA segmentation methods [tendon core+tendon paratenon (Maganaris and Paul, 2002; Magnusson and Kjaer, 2003; Reeves and Cooper, 2017); only tendon core (present study)] and tendon region from which the measurement of tendon CSA was made [free AT insertion (Maganaris and Paul, 2002); whole free AT length (present study)]. Further, resting free AT volume in the tendinopathic and contralateral legs was 7.16 and 4.15 ml, respectively. These values fall within the range reported in previous *in vivo* studies for free AT volume [tendinopathic free AT volume: ∼6–8 ml (Shalabi et al., 2004; Gärdin et al., 2010); healthy free AT volume: ∼3–5 ml (Obst et al., 2014a,b; Nuri et al., 2016)]. As no significant differences in free AT length were found between the tendinopathic and contralateral legs at rest (∼72 mm), the higher volume of the free tendon in the tendinopathic leg observed here reflects the larger CSA of the tendinopathic tendon as a result of pathological alterations in tendon structure and composition accompanying chronic MAT (Åström and Rausing, 1995; Docking et al., 2015).

### Longitudinal and transverse strain of the AT during repeated loading

AT longitudinal and transverse strain from the first to tenth contraction were 3 and 5 times greater in the tendinopathic AT compared with the contralateral tendon. The longitudinal creep of whole AT was primarily driven from the free AT in the MAT and contralateral tendons, with no differences in tendon proximal AT strain observed between contractions and between tendons during repeated loads. This finding adds to previous studies that reported a higher longitudinal strain at the level of the whole (Arya and Kulig, 2010; Child et al., 2010) and free tendon in MAT relative to the healthy control tendon, by showing that the strain behaviour of the proximal AT is not affected in MAT and does not experience longitudinal creep in response to repeated loading. The proximal AT therefore does not appear to be vulnerable to strain-related injuries during repeated loading in MAT. Differences in tendon anatomical structure [fascicle/fibre orientation (Szaro et al., 2009), fluid content (Grosse et al., 2016) and crimp angle (Magnusson et al., 2002)], the magnitude and direction of the load exerted, and loading distribution pattern (Iwanuma et al., 2011; Farris et al., 2013; Reeves and Cooper, 2017) between proximal AT and free AT have been proposed as possible mechanisms underpinning the isolated creep behaviour of the free AT during repeated loading (Nuri et al., 2016).

### Volumetric changes of the free AT during repeated loading

In contrast to normal tendon, which is known to behave iso-volumetrically in response to repeated loads (Nuri et al., 2016), the present study revealed that the free AT core experienced a volume reduction of 29% by the tenth contraction in MAT. This finding is consistent with studies that report reduction in tendinopathic tendon water content (Ho and Kulig, 2016), volume (Shalabi et al., 2004) and thickness (Fahlström and Alfredson, 2010; Grigg et al., 2012; Wearing et al., 2015) following exercise. The gradual increase in tendinopathic free AT length and the corresponding reduction in tendon CSA and volume observed here suggests that repeated loading not only changes a tendinopathic free AT matrix shape but also alters tendon fluid content until a steady state is reached. We also noted that despite the volume and CSA reduction loss in the tendinopathic tendon during repeated loading, the free AT volume and CSA remained higher (5.12 ml and 67 $mm^2$, respectively) compared with those in the contralateral tendon (4.15 ml and 55 $mm^2$, respectively) following repeated loading. The volume reduction in MAT under load therefore does not fully account for the extra volume in the resting tendon due to pathology. From an injury prevention perspective, the larger CSA in MAT would be expected to protect the tendon from experiencing high stress and compensate at least in part for the lower tendon material properties (Arya and Kulig, 2010; Child et al., 2010; Wang et al., 2012; Chang and Kulig, 2015).

The load-induced volume reduction of the tendinopathic free tendon during repeated loads as observed here could be due to fluid movement from the tendon core to the peri-tendinous space (Hannafin and Arnoczky, 1994; Helmer et al., 2004) and/or vascular mechanism (i.e. the contraction-induced decrease in tendinopathic tendon blood volume) (Åström and Westlin, 1994). The fluid movement from the tendon core to the peri-tendinous space during mechanical loading could be explained by a combination of factors such as the release of water molecules from glycosaminoglycans as a result of the induced electric potential, known as streaming potential (Gu et al., 1993), in the tendinopathic tendon matrix and high positive fluid pressure in the tendinopathic tendon core (Ahmadzadeh et al., 2015) resulting from the high concentration of free and bound water molecules (De Mos et al., 2007) and ineffective tendon loading transfer mechanisms due to the disorganized and disrupted collagen fibres (Pingel et al., 2014) within the tendinopathic tendon matrix. The impairment in tendinopathic tendon core sheath (i.e. epitenon) permeability (i.e. porosity and void ratio) (Chen et al., 1998) could also exacerbate the effect of the aforementioned mechanisms.

### Number of contractions required to achieve steady-state AT strain behaviour

Steady-state behaviour was achieved simultaneously for longitudinal and transverse AT strains following five contractions in the tendinopathic tendon compared with three contractions in the contralateral tendon. More contractions were probably required on the tendinopathic side because of a combination of more longitudinal and transverse creep coupled with the volume reduction in MAT. We also observed a reduction in self-reported pain score up to the third contraction in MAT, which probably reflects changes in the local mechanical environment within the tendinopathic tendon matrix during repeated loading. A practical implication of these findings is that more contractions are required to condition a tendon with MAT relative to a healthy tendon, and that tendon conditioning in MAT has the added benefit of decreasing pain perception (Rio et al., 2015).

Although the tendinopathic tendon underwent significantly greater CSA and corresponding volume reduction than the contralateral tendon from the first contraction, the whole and free AT longitudinal strain on the tendinopathic side were not greater than those of the contralateral tendon until the fourth contraction. This observation could be attributed to the involvement of different

load-bearing mechanisms at different time scales within the tendinopathic tendon matrix in response to repetitive tensile loading. It is well known that the load support mechanisms of the tendon derive from the simultaneous interaction of the solid and fluid phases of the tissue (Fung, 2013) and that the tendinopathic tendon has a degraded solid structure (Pingel et al., 2014; Docking et al., 2015) and contains more free and bound water molecules (De Mos et al., 2007). The normal fluid–solid interaction pattern within the tendon in response to load in the presence of tendinopathy appears to be altered, with the rapid volume reduction from the free AT core observed in MAT being suggestive of a decreasing support from the fluid component and a corresponding increase in load bearing to the solid component until steady state is reached. The specific reason for the lack of statistical difference in free AT longitudinal strain between the tendinopathic tendon and contralateral tendon in the first three contractions is unclear, but it could be caused by a stiffening effect of fluid flow on the more compliant collagen fibrillar network in MAT (Buckley et al., 2013). These alterations in solid and fluid behaviour in MAT would also be expected to alter the local mechanical environment of the tissue. A non-optimal mechanical environment within the free tendon in MAT could be an important factor limiting tendon regeneration, and may need to be considered when designing interventions for treating MAT.

## Limitations and future directions

In the present study, only the mean whole free AT transverse strain was assessed because of the large variation in tendon injury location along the length of the free AT in participants with MAT. Studies in the field of tendon mechanobiology suggest that there is an optimal strain environment for positive tendon adaptation (Wang, 2006), with either higher or lower than optimal strains resulting in a catabolic effect. It therefore follows that targeted rehabilitation strategies, perhaps combining biological and exercise-based therapies, could be developed in the future to create an optimal mechanical environment for tendon regeneration. In future studies, it will be important to better characterize the local strains in the region of the tendinopathic lesion. Additionally, we were not able to visualize the whole tendon CSA along the proximal AT during a single transverse ultrasound sweep in the present study. Such information could be obtained in future using other imaging approaches such as MRI (Iwanuma et al., 2011; Reeves and Cooper, 2017). Furthermore, 3D US is limited by its inability to detect the thickness of the tendon paratenon, epitenon and peri-tendinous space, and thus the tendon CSA measurement in the present study was confined to the tendon core. Additional studies are required to determine these tendon parameters at rest and during repeated loading using imaging techniques such as MRI that have greater resolution than ultrasound in order to identify the fluid exudation mechanism from the tendon core into the peri-tendinous space as well as the time course of recovery of tendinopathic tendon volume following a standardized AT repeated loading protocol. Also, although all measurements were made at the same relative ankle joint plantarflexion torque (50% MVIC), we cannot be certain that the force applied to the free tendon and proximal AT was equal or whether longitudinal and/or transverse force distribution changed as a function of contraction number. It is, however, important to note that the activation level of TA muscle during repeated isometric plantarflexion contractions was small (~5%) and no changes in EMG activity of the TS and TA muscles and the co-activation index were detected between contractions. Finally, the present study was conducted using a specific repeated loading protocol (25 s at 50% MVIC per contraction) (Nuri et al., 2016) in male adults with unilateral MAT so caution should be taken when generalizing these findings to other loading protocols (high-intensity–short-duration loading), females, other AT disorders (e.g. insertional Achilles tendinopathy) and other tendons (e.g. patellar tendon).

## Conclusion

Tendinopathic free AT underwent higher longitudinal, transverse and volume strains relative to the contralateral tendon and reached steady-state strain behaviour after a greater number of contractions. The loss of free AT volume in MAT preceded the greater longitudinal strain in MAT relative to the contralateral tendon. Taken together, these findings suggest the 3D strain behaviour and normal temporal pattern of interaction between the solid and fluid phases of the tissue within the tendinopathic tendon matrix are altered in response to repeated loading.

### Competing interests

The authors declare no competing or financial interests.

### Author contributions

Conceptualization: L.N., S.J.O., R.N.-W., R.S.B.; Methodology: L.N.; Formal analysis: L.N., R.S.B.; Investigation: L.N.; Resources: L.N.; Writing - original draft: L.N.; Writing - review & editing: L.N., S.J.O., R.N.-W., R.S.B.; Supervision: S.J.O., R.N.-W., R.S.B.

### Funding

This research received no specific grant from any funding agency in the public, commercial or not-for-profit sectors.

### Data availability

Data are available from the Dryad Digital Repository (Nuri et al., 2017): http://dx.doi.org/10.5061/dryad.3n15h

### References

**Ahmadzadeh, H., Freedman, B. R., Connizzo, B. K., Soslowsky, L. J. and Shenoy, V. B.** (2015). Micromechanical poroelastic finite element and shear-lag models of tendon predict large strain dependent Poisson's ratios and fluid expulsion under tensile loading. *Acta Biomater.* **22**, 83-91.

**Alfredson, H., Pietilä, T., Jonsson, P. and Lorentzon, R.** (1998). Heavy-load eccentric calf muscle training for the treatment of chronic Achilles tendinosis. *Am. J. Sports Med.* **26**, 360-366.

**Arya, S. and Kulig, K.** (2010). Tendinopathy alters mechanical and material properties of the Achilles tendon. *J. Appl. Physiol.* **108**, 670-675.

**Åström, M. and Rausing, A.** (1995). Chronic Achilles Tendinopathy: a survey of surgical and histopathologic findings. *Clin. Orthop. Relat. Res.* **316**, 151-164.

**Åström, M. and Westlin, N.** (1994). Blood flow in chronic Achilles tendinopathy. *Clin. Orthop. Relat. Res.* **308**, 166-172.

**Buckley, M. R., Sarver, J. J., Freedman, B. R. and Soslowsky, L. J.** (2013). The dynamics of collagen uncrimping and lateral contraction in tendon and the effect of ionic concentration. *J. Biomech.* **46**, 2242-2249.

**Chang, Y.-J. and Kulig, K.** (2015). The neuromechanical adaptations to Achilles tendinosis. *J. Physiol.* **593**, 3373-3387.

**Chen, C. T., Malkus, D. S. and Vanderby, R., Jr**. (1998). A fiber matrix model for interstitial fluid flow and permeability in ligaments and tendons. *Biorheology* **35**, 103-118.

**Child, S., Bryant, A. L., Clark, R. A. and Crossley, K. M.** (2010). Mechanical properties of the Achilles tendon aponeurosis are altered in athletes with achilles tendinopathy. *Am. J. Sports. Med.* **38**, 1885-1893.

**De Jonge, S., Van Den Berg, C., De Vos, R. J., Van Der Heide, H. J. L., Weir, A., Verhaar, J. A. N., Bierma-Zeinstra, S. M. A. and Tol, J. L.** (2011). Incidence of midportion Achilles tendinopathy in the general population. *Br. J. Sports. Med.* **45**, 1026-1028.

**De Mos, M., Van El, B., DeGroot, J., Jahr, H., Van Schie, H. T. M., Van Arkel, E. R., Tol, H., Heijboer, R., Van Osch, G. J. V. M. and Verhaar, J. A. N.** (2007). Achilles tendinosis: changes in biochemical composition and collagen turnover rate. *Am. J. Sports. Med.* **35**, 1549-1556.

**Debenham, J. R., Travers, M. J., Gibson, W., Campbell, A. and Allison, G. T.** (2016). Achilles tendinopathy alters stretch shortening cycle behaviour during a sub-maximal hopping task. *J. Sci. Med. Sport.* **19**, 69-73.

**Docking, S. I. and Cook, J.** (2016). Pathological tendons maintain sufficient aligned fibrillar structure on ultrasound tissue characterization (UTC). *Scand. J. Med. Sci. Sports* **26**, 675-683.

**Docking, S. I., Rosengarten, S. D., Daffy, J. and Cook, J.** (2015). Structural integrity is decreased in both Achilles tendons in people with unilateral Achilles tendinopathy. *J. Sci. Med. Sport* **18**, 383-387.
**Fahlström, M. and Alfredson, H.** (2010). Ultrasound and Doppler findings in the Achilles tendon among middle-aged recreational floor-ball players in direct relation to a match. *Br. J. Sports Med.* **44**, 140-143.
**Farris, D. J., Trewartha, G., McGuigan, M. P. and Lichtwark, G. A.** (2013). Differential strain patterns of the human Achilles tendon determined in vivo with freehand three-dimensional ultrasound imaging. *J. Exp. Biol.* **216**, 594-600.
**Fung, Y. C.** (2013). *Biomechanics: Mechanical Properties of Living Tissues*. New York: Springer-Verlag.
**Gärdin, A., Movin, T., Svensson, L. and Shalabi, A.** (2010). The long-term clinical and MRI results following eccentric calf muscle training in chronic Achilles tendinosis. *Skeletal. Radiol.* **39**, 435-442.
**Grigg, N. L., Wearing, S. C. and Smeathers, J. E.** (2012). Achilles tendinopathy has an aberrant strain response to eccentric exercise. *Med. Sci. Sports. Exerc.* **44**, 12-17.
**Grosse, U., Syha, R., Gatidis, S., Grozinger, G., Martirosian, P., Partovi, S., Nikolaou, K., Robbin, M. R., Schick, F. and Springer, F.** (2016). MR-based in vivo follow-up study of Achilles tendon volume and hydration state after ankle-loading activity. *Scand. J. Med. Sci. Sports* **26**, 1200-1208.
**Gu, W. Y., Lai, W. M. and Mow, V. C.** (1993). Transport of fluid and ions through a porous-permeable charged-hydrated tissue, and streaming potential data on normal bovine articular cartilage. *J. Biomech.* **26**, 709-723.
**Hammond, M. C., Fitts, S. S., Kraft, G. H., Nutter, P. B., Trotter, M. J. and Robinson, L. M.** (1988). Co-contraction in the hemiparetic forearm: quantitative EMG evaluation. *Arch. Phys. Med. Rehabil.* **69**, 348-3451.
**Hannafin, J. A. and Arnoczky, S. P.** (1994). Effect of cyclic and static tensile loading on water content and solute diffusion in canine flexor tendons: an in vitro study. *J. Orthop. Res.* **12**, 350-356.
**Hansen, W., Shim, V. B., Obst, S., Lloyd, D. G., Newsham-West, R. and Barrett, R. S.** (2017). Achilles tendon stress is more sensitive to subject-specific geometry than subject-specific material properties: a finite element analysis. *J. Biomech.* **56**, 26-31.
**Hawkins, D., Lum, C., Gaydos, D. and Dunning, R.** (2009). Dynamic creep and pre-conditioning of the Achilles tendon *in-vivo*. *J. Biomech.* **42**, 2813-2817.
**Helmer, K. G., Wellen, J., Grigg, P. and Sotak, C. H.** (2004). Measurement of the spatial redistribution of water in rabbit Achilles tendon in response to static tensile loading. *J. Biomech. Eng.* **126**, 651-656.
**Hermens, H. J., Freriks, B., Disselhorst-Klug, C. and Rau, G.** (2000). Development of recommendations for SEMG sensors and sensor placement procedures. *J. Electromyogr. Kinesiol.* **10**, 361-374.
**Ho, K.-Y. and Kulig, K.** (2016). Changes in water content in response to an acute bout of eccentric loading in a patellar tendon with a history of tendinopathy: a case report. *Physiother. Theory. Pract.* **32**, 566-570.
**Iwanuma, S., Akagi, R., Kurihara, T., Ikegawa, S., Kanehisa, H., Fukunaga, T. and Kawakami, Y.** (2011). Longitudinal and transverse deformation of human Achilles tendon induced by isometric plantar flexion at different intensities. *J. Appl. Physiol.* **110**, 1615-1621.
**Kvist, M.** (1994). Achilles tendon injuries in athletes. *Sports Med.* **18**, 173-201.
**Leung, J. L. Y. and Griffith, J. F.** (2008). Sonography of chronic Achilles tendinopathy: a case–control study. *J. Clin. Ultrasound.* **36**, 27-32.
**Lichtwark, G. A., Cresswell, A. G. and Newsham-West, R. J.** (2013). Effects of running on human Achilles tendon length–tension properties in the free and gastrocnemius components. *J. Exp. Biol.* **216**, 4388-4394.
**Maffulli, N., Khan, K. M. and Puddu, G.** (1998). Overuse tendon conditions: time to change a confusing terminology. *Arthroscopy* **14**, 840-843.
**Maganaris, C. N.** (2003). Tendon conditioning: artefact or property? *Proc. Biol. Sci.* **270**, S39-S42.
**Maganaris, C. N. and Paul, J. P.** (2002). Tensile properties of the in vivo human gastrocnemius tendon. *J. Biomech.* **35**, 1639-1646.
**Magnusson, S. P. and Kjaer, M.** (2003). Region-specific differences in Achilles tendon cross-sectional area in runners and non-runners. *Eur. J. Appl. Physiol.* **90**, 549-553.
**Magnusson, S. P., Qvortrup, K., Larsen, J. O., Rosager, S., Hanson, P., Aagaard, P., Krogsgaard, M. and Kjaer, M.** (2002). Collagen fibril size and crimp morphology in ruptured and intact Achilles tendons. *Matrix. Biol.* **21**, 369-377.
**Nuri, L., Obst, S. J., Newsham-West, R. and Barrett, R. S.** (2016). Regional three-dimensional deformation of human Achilles tendon during conditioning. *Scand. J. Med. Sci. Sports*.
**Nuri, L., Obst, S. J., Newsham-West, R. and Barrett, R. S.** (2017). Data from: The tendinopathic Achilles tendon does not remain iso-volumetric upon repeated loading: insights from 3D ultrasound. Dryad Digital Repository. http://dx.doi.org/10.5061/dryad.3n15h
**Obst, S. J., Newsham-West, R. and Barrett, R. S.** (2014a). In vivo measurement of human Achilles tendon morphology using freehand 3-D ultrasound. *Ultrasound Med. Biol.* **40**, 62-70.
**Obst, S. J., Renault, J.-B., Newsham-West, R. and Barrett, R. S.** (2014b). Three-dimensional deformation and transverse rotation of the human free Achilles tendon in vivo during isometric plantarflexion contraction. *J. Appl. Physiol.* **116**, 376-384.
**Obst, S. J., Newsham-West, R. and Barrett, R. S.** (2015). Three-dimensional morphology and strain of the human Achilles free tendon immediately following eccentric heel drop exercise. *J. Exp. Biol.* **218**, 3894-3900.
**Pingel, J., Lu, Y., Starborg, T., Fredberg, U., Langberg, H., Nedergaard, A., Weis, M. A., Eyre, D., Kjaer, M. and Kadler, K. E.** (2014). 3-D ultrastructure and collagen composition of healthy and overloaded human tendon: evidence of tenocyte and matrix buckling. *J. Anat.* **224**, 548-555.
**Prager, R. W., Rohling, R. N., Gee, A. H. and Berman, L.** (1998). Rapid calibration for 3-D freehand ultrasound. *Ultrasound Med. Biol.* **24**, 855-869.
**Reeves, N. D. and Cooper, G.** (2017). Is human Achilles tendon deformation greater in regions where cross-sectional area is smaller? *J. Exp. Biol.* **220**, 1634-1642.
**Rio, E., Kidgell, D., Purdam, C., Gaida, J., Moseley, G. L., Pearce, A. J. and Cook, J.** (2015). Isometric exercise induces analgesia and reduces inhibition in patellar tendinopathy. *Br. J. Sports Med.* **49**, 1277-1283.
**Shalabi, A., Kristoffersen-Wilberg, M., Svensson, L., Aspelin, P. and Movin, T.** (2004). Eccentric training of the gastrocnemius-soleus complex in chronic Achilles tendinopathy results in decreased tendon volume and intratendinous signal as evaluated by MRI. *Am. J. Sports Med.* **32**, 1286-1296.
**Smith, D. W., Rubenson, J., Lloyd, D., Zheng, M., Fernandez, J., Besier, T., Xu, J. and Gardiner, B. S.** (2013). A conceptual framework for computational models of Achilles tendon homeostasis. *Wiley. Interdiscip. Rev. Syst. Biol. Med.* **5**, 523-538.
**Szaro, P., Witkowski, G., Śmigielski, R., Krajewski, P. and Ciszek, B.** (2009). Fascicles of the adult human Achilles tendon–an anatomical study. *Ann. Anat.* **191**, 586-593.
**Treece, G. M., Prager, R. W., Gee, A. H. and Berman, L.** (1999). Fast surface and volume estimation from non-parallel cross-sections, for freehand three-dimensional ultrasound. *Med. Image Anal.* **3**, 141-173.
**Van Dijk, C. N., Van Sterkenburg, M. N., Wiegerinck, J. I., Karlsson, J. and Maffulli, N.** (2011). Terminology for Achilles tendon related disorders. *Knee. Surg. Sports Traumatol. Arthrosc.* **19**, 835-841.
**Wang, J. H.-C.** (2006). Mechanobiology of tendon. *J. Biomech.* **39**, 1563-1582.
**Wang, H.-K., Lin, K.-H., Su, S.-C., Shih, T. T.-F. and Huang, Y.-C.** (2012). Effects of tendon viscoelasticity in Achilles tendinosis on explosive performance and clinical severity in athletes. *Scand. J. Med. Sci. Sports* **22**, e147-e155.
**Wearing, S. C., Locke, S., Smeathers, J. E. and Hooper, S. L.** (2015). Tendinopathy alters cumulative transverse strain in the patellar tendon after exercise. *Med. Sci. Sports Exerc.* **47**, 264-271.